A polymer-based interface restores light sensitivity in blind rat retinas

Diego Ghezzi[1], Maria Rosa Antognazza[2], Rita Maccarone[3], Sebastiano Bellani[2], Erica Lanzarini[2], Nicola Martino[2], Maurizio Mete[4], Grazia Pertile[4], Silvia Bisti[3], Guglielmo Lanzani[2,*], Fabio Benfenati[1,5,*]

[1]Department of Neuroscience and Brain Technologies, Istituto Italiano di Tecnologia, Genova, Italy; [2]Center for Nano Science and Technology@PoliMi, Istituto Italiano di Tecnologia, Milano, Italy; [3]Dipartimento di Tecnologie Biomediche, Università dell'Aquila, L'Aquila, Italy; [4]UO Oculistica, Ospedale S. Cuore-Don Calabria, Negrar, Italy; [5]Department of Experimental Medicine, University of Genova, Genova, Italy.

* e-mail: guglielmo.lanzani@iit.it and fabio.benfenati@iit.it

Supplementary Methods

Cell Culture. Primary cultures of hippocampal neurons were prepared from embryonic day 18 embryos of pregnant Sprague-Dawley rats (Charles River). Briefly, hippocampi were dissociated by a 15 min incubation with 0.25% trypsin at 37 °C, and cells were plated at a density of 200 cells/mm^2 on poly-L-lysine (0.1 mg/ml)-treated organic layers and control substrates in Neurobasal medium (Invitrogen) supplemented with 10% horse serum (Hyclone). After allowing neurons to adhere to the surface for 3-4 hr, cells were cultured in serum-free Neurobasal medium supplemented with 2 % B27 (Invitrogen) and 2 mM glutamine (Invitrogen).

Cell viability assay. Cell viability was verified by propidium iodine/fluorescein diacetate staining at 21 DIV. Attached cells were rinsed twice with recording extracellular solution and incubated for 4 min in the same solution containing 15 µg/ml of fluorescein diacetate, 5 µg/ml of propidium iodine and 3 µg/ml of Hoechst-33342 (Sigma-Aldrich). Cells were washed with recording extracellular solution, and multiple images were acquired with a C91006 CCD camera (Hamamatsu Photonics). Standard 4'-6-diamidino-2-phenylindole (ex: D350/50x, em: D460/50m, dic: 400dclp), fluorescein isothiocyanate (ex: D480/30x, em: D535/40m, dic: 505dclp) and tetramethylrhodamine isothiocyanate (ex: D540/25x, em: D605/55m, dic: 565dclp) filter sets were used to image Hoechst-33342, fluorescein diacetate and propidium iodine, respectively. Images were taken from neurons cultured both on organic layers (n = 6) and control substrates (n = 6). Five fields per substrate were imaged, and the percentages of living and dead cells per field were counted and averaged. The percentage of healthy cells was calculated as the percentage of fluorescein diacetate-positive cells over the total number of nuclei stained by Hoechst-33342. As a control, the percentage of dead cells was computed as the percentage of apoptotic cells (identified by Hoechst-33342) and necrotic cells (identified by propidium iodine) over the total number of Hoechst-33342-positive nuclei.

Confocal imaging. At 4 weeks after the induction of photoreceptor degeneration, retinas were examined in sections labelled for nuclear structures. After the animals were euthanised, each eye was dissected free. The superior aspect of the eye was marked with a pen, and the eyes were fixed by immersion in 4 % paraformaldehyde fixative buffer at 4 °C for 3 hr. Eyes were rinsed three times in 0.1 M phosphate-buffered saline and left overnight in a 15% sucrose solution to provide cryoprotection. Eyes were embedded in mounting medium (Tissue-Tek OCT compound; Sakura Finetek) by snap freezing in liquid nitrogen. Sections were cut at 20 µm along the vertical meridian of the eye to produce sections that extended from the superior to the inferior edge. Sections were mounted on gelatin and poly-L-lysine-coated slides, dried overnight in a 50 °C oven and stored at -20 °C until processing. Retinal sections were labelled with the nuclear stain bisbenzimide and acquired on a confocal laser-scanning microscope (TCS SP5; Leica Microsystems)[1].

Polymeric film characterisation. *Absorption measurements* were performed using a PERKIN ELMER Spectrophotometer (Lambda 1040), and the *thicknesses* of the active layer were determined by

profilometry (KLA TENCOR, Alpha Step 500). *External Quantum Efficiency* was defined as SR(λ) hc / λe, where SR(λ) is the spectral responsivity (i.e., the photocurrent action spectrum properly corrected by the light incident spectrum, the device area and the reference detector responsivity), h is the Planck constant, c is the velocity of light, λ is the wavelength, and e is the electronic charge. This efficiency value was measured by illuminating the samples with a tungsten halogen light source (Oriel) that was spectrally filtered by a Cornerstone 260 1/4M monochromator (Oriel) and by acquiring the photocurrent signal with a lock-in technique (MERLIN digital radiometry system). *Photoluminescence spectra* were acquired using a JOBIN-YVON spectrofluorometer; the excitation wavelength was set at 520 nm, and the acquisition time was 3 s. All samples were prepared in a glove box. The first sample set was kept under a nitrogen atmosphere in the dark, except for the short measurement time, and the second set was kept in contact with a saline solution (NaCl, 200 mM) and continuously illuminated (12 hr). *Measurements of the contact angle* before and after immersion in saline solution (NaCl, 200 mM) were obtained using a dedicated instrument (DATAPHYSICS, OCA-15) and distilled water drops (2 µl) as a reference. Samples were realised in a glove-box under a controlled atmosphere. Prior to immersion, the samples were measured immediately after exposure to air. Changes in contact angles were measured in samples kept in contact with the saline electrolyte for more than 20 hr under continuous white light illumination and under closed-circuit conditions. *Capacitance vs. voltage characterisations* were performed in saline solution (NaCl, 200 mM) using a potentiostat (METROHM Autolab PGstat 302) working in a two-electrode configuration. The working electrode (P3HT/ITO thin film) and the reference electrode (Pt planar sheet) were of comparable dimensions, on the order of 1 cm^2. All measurements were carried out in the dark and at room temperature. Data analyses were performed using NOVA 1.8 software. The dopant concentration, N_A, was extrapolated using the following relation (the Mott-Schottky equation): $C^{-2} = 2 (V_{sc}) / A^2 e\varepsilon_r\varepsilon_0 N_A$, where V_{sc} is the potential drop inside the semiconductor, which depends on the externally applied potential difference V, A is the polymer area (~ 1.5 cm^2), e is the electronic charge and ε_r and ε_0 are the medium and the vacuum dielectric permittivities, respectively.

Statistical analyses and data rendering. Statistical analyses were performed using SigmaPlot (Systat Software), and data were plotted using OriginPro (OriginLab Corporation). Data were compared by one-way ANOVA followed by post-hoc multiple comparison tests or, in the case of two experimental groups, by Student's *t*-test. The error bars and ± values represent the s.e.m.

Supplementary Results

Interface modelling

The data reported in sections "Interface characterisation" and "Photo-stimulation of primary neurons" are consistent with the creation of a negatively charged layer at the polymer/electrolyte interface upon photo-stimulation. The ion displacement phenomena leading to neuronal stimulation may be due either to a capacitive coupling between the accumulated negative charges and the outer cell membrane or to electron transfer phenomena that give rise to faradaic currents in the thin cleft between the polymer surface and the neuronal membrane. We thus performed a set of measurements to characterise the properties of the polymer layer in contact with the electrolyte. The presence of the electrolyte strongly influenced the physical/chemical properties of the polymer such that new processes, different from those in the reported literature for pristine films under a controlled atmosphere[2], became relevant. When P3HT is brought into contact with the electrolyte, diffusion processes may enhance the *p*-type doping (a phenomenon that usually occurs when polymer films are exposed to air), which possibly adds a further degree of contamination. To test this hypothesis, we measured both absorbance and photoluminescence of the polymer film under prolonged contact with the electrolyte and upon illumination. We found that, under these conditions, the photoluminescence efficiency dropped dramatically, while the absorbance was only slightly affected (**Supplementary Fig. 6a**). This finding is consistent with reactions with electrolyte contaminants that generate new acceptor states. The shapes and the increasing slopes of voltage-capacitance curves (**Supplementary Fig. 6b**) that were recorded under dark conditions at various wetting times confirmed the increase of the *p*-doping level in the P3HT polymer film (**Supplementary Fig. 6c**). This finding may have been due to molecular oxygen that caused oxidation of the polymer, thereby leaving free positive polarons and trapped negative ions (O_2^-)[3]. Contact angle measurements (**Supplementary Fig. 6d**) further corroborated the surface contamination by showing that the hydrophobic character of the polymer was reduced as the time in contact with the electrolyte was increased[4,5].

Finally, **Supplementary Fig. 6e** shows External Quantum Efficiency (EQE) spectra measured in the electrochemical cell ITO/P3HT/electrolyte for illumination from both sides of the device. Although the photocurrent was measured across the device by closing the circuit on an external load (i.e. a configuration that was different from that used for neuron stimulation), this approach can provide useful information about the polymer state. A symbatic behaviour (i.e., one closely resembling the optical absorption spectrum, **Supplementary Fig. 6a**) was observed for light impinging on ITO, and an antibatic behaviour[6] was observed for light impinging through the electrolyte. This finding excluded efficient bulk photogeneration and suggested that charge carriers contributing to the external current were mainly formed at the polymer/ITO interface.

Based on previous studies[7-11] and reported characterisation, a scenario for the polymer/electrolyte system could be drawn. Opposite to standard organic photovoltaic cells, the high levels of doping (**Supplementary**

Fig. 6a-d) led to the formation of charged layers at the polymer boundary that screen the internal electric field. For this reason, no driving force was present in the polymer bulk, and the photo-generated polarons could not be spatially separated and rapidly recombined before being extracted. The EQE measurements (**Supplementary Fig. 6e**) demonstrated that the polymer/ITO interface plays a fundamental role in the charge dissociation process. Upon photo-stimulation, the anodic contact acts as a hole sink, leaving the polymer layer negatively charged. As a consequence, positive ions accumulate at the polymer surface, thereby leaving a diffuse negative layer in the electrolyte (Helmholtz double layer[8]). This scenario is consistent with the results reported in **Fig. 1** and provides evidence for a capacitive coupling between the polymer and the extracellular medium that leads to neuronal photo-stimulation.

Supplementary References

1 Natoli, R. *et al.* Gene and noncoding RNA regulation underlying photoreceptor protection: microarray study of dietary antioxidant saffron and photobiomodulation in rat retina. *Molecular vision* **16**, 1801-1823 (2010).

2 Bisquert, J. *et al.* Band unpinning and photovoltaic model for P3HT:PCBM organic bulk heterojunctions under illumination. *Chem Phys Lett* **465**, 57-62 (2008).

3 Sharma, A., Mathijssen, S. G. J., Kemerink, M., de Leeuw, D. M. & Bobbert, P. A. Proton migration mechanism for the instability of organic field-effect transistors. *Appl Phys Lett* **95** (2009).

4 Lin, P., Yan, F. & Chan, H. L. W. Improvement of the Tunable Wettability Property of Poly(3-alkylthiophene) Films. *Langmuir* **25**, 7465-7470 (2009).

5 Scarpa, G., Idzko, A. L., Gotz, S. & Thalhammer, S. Biocompatibility Studies of Functionalized Regioregular Poly(3-hexylthiophene) Layers for Sensing Applications. *Macromol Biosci* **10**, 378-383 (2010).

6 Antognazza, M. R., Musitelli, D., Perissinotto, S. & Lanzani, G. Spectrally selected photodiodes for colorimetric application. *Org Electron* **11**, 357-362 (2010).

7 Bystrenova, E. *et al.* Neural networks grown on organic semiconductors. *Adv Funct Mater* **18**, 1751-1756 (2008).

8 Bard, A. J. & Faulkner, L. R. Electrochemical methods: fundamentals and applications. *Wiley New York* **2** (1980).

9 Gautam, V., Bag, M. & Narayan, K. S. Single-Pixel, Single-Layer Polymer Device as a Tricolor Sensor with Signals Mimicking Natural Photoreceptors. *J Am Chem Soc* **133**, 17942-17949 (2011).

10 Ghezzi, D. *et al.* A hybrid bioorganic interface for neuronal photoactivation. *Nature Communications* **2** (2011).

11 Widge, A. S., Jeffries-El, M., Cui, X. Y., Lagenaur, C. F. & Matsuoka, Y. Self-assembled monolayers of polythiophene conductive polymers improve biocompatibility and electrical impedance of neural electrodes. *Biosens Bioelectron* **22**, 1723-1732 (2007).

Supplementary Figures

Supplementary Figure 1

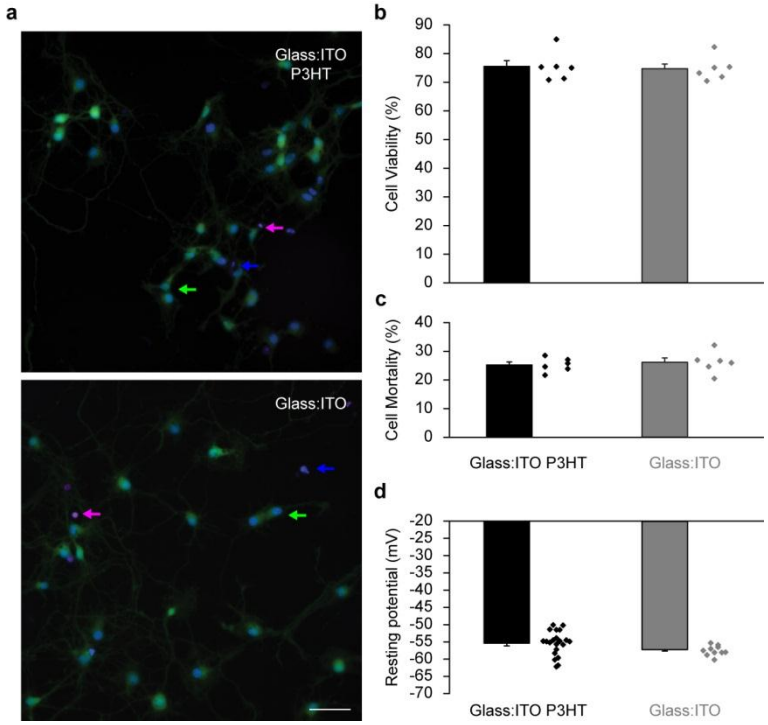

Supplementary Figure 1 | Effect of the P3HT active layer on the cell viability of hippocampal neurons. (**a**) Propidium iodine/fluorescein diacetate staining assay performed at 21 DIV. Green, blue and violet arrows indicate viable, apoptotic and necrotic/apoptotic cells, respectively. Scale bar: 25 µm. (**b**) Comparison of the mean (± s.e.m.) cell viability on either P3HT-coated Glass:ITO (black) or control Glass:ITO (grey) substrates at 21 DIV (Student's *t*-test, P = 0.818, *n* = 6). (**c**) Comparison of the mean (± s.e.m.) cell mortality on either P3HT-coated Glass:ITO (black) or control Glass:ITO (grey) substrates at 21 DIV (Student's *t*-test, P = 0.639, *n* = 6). (**d**) Comparison of the mean (± s.e.m.) resting membrane potential of neurons cultured on either P3HT-coated Glass:ITO (black, *n* = 21) or control Glass:ITO (grey, *n* = 10) substrates. This analysis did not reveal any significant difference (Student's *t*-test, P = 0.128).

Supplementary Figure 2

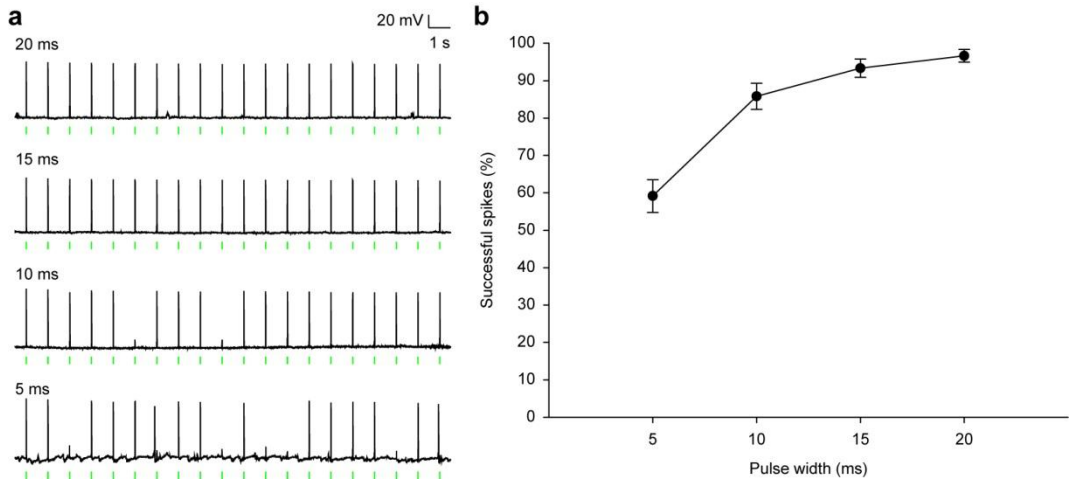

Supplementary Figure 2 | Effect of the duration of the light pulse on spike generation by hippocampal neurons over a P3HT active layer. (**a**) Neuronal activation was recorded at various pulse widths with a train of 20 pulses delivered at 1 Hz (green bars). (**b**) The percentage of successful spikes in the train was computed over all recorded neurons and is reported as a function of the pulse width (*n* = 7, means ± s.e.m.).

Supplementary Figure 3

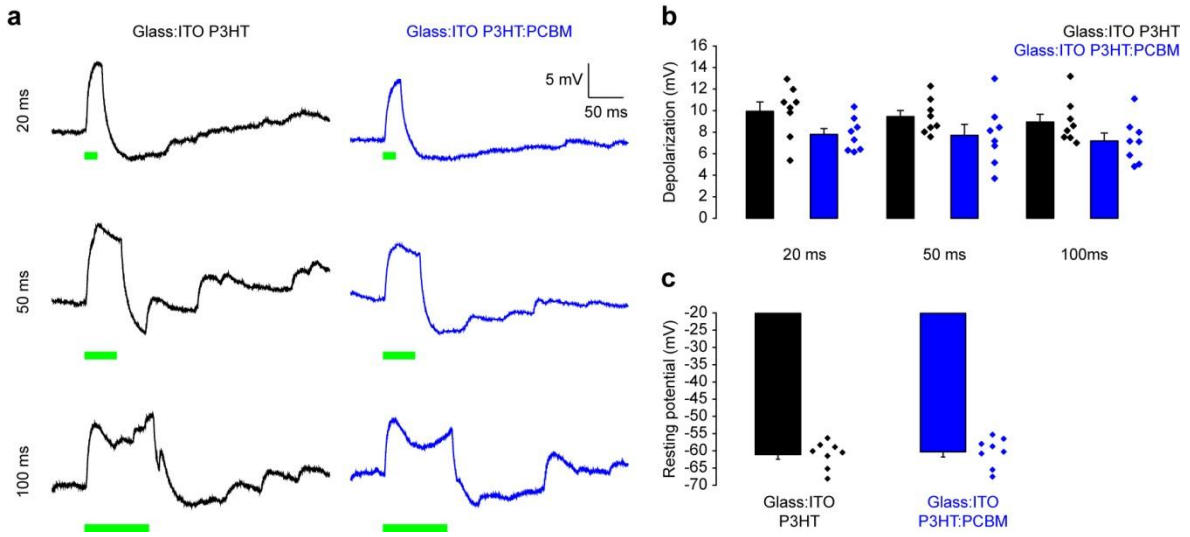

Supplementary Figure 3 | Comparison of neuronal depolarisation induced by illumination of P3HT and P3HT:PCBM active layers. (**a**) Amplitude of the depolarisation recorded in neurons cultured over either P3HT-coated Glass:ITO (black, *n* = 8) or P3HT:PCBM-coated Glass:ITO (blue, *n* = 8) substrates for light pulses (green bars) of increasing duration (20 ms, 50 ms and 100 ms; 15 mW/mm^2) in the presence of TTX (1 µM). Traces represent the means of five consecutive sweeps. (**b**) Comparison of the mean (± s.e.m.) amplitudes of depolarisation for neurons cultured under the conditions described in **a.** The analysis did not show any significant difference between the two interfaces (20 ms pulse: P = 0.053, 50 ms: P = 0.155, 100 ms: P = 0.108, Student's *t*-test). (**c**) Comparison of the mean (± s.e.m.) resting membrane potentials of neurons cultured under the conditions described in **a.** No significant differences were found (Student's *t*-test, P = 0.703).

Supplementary Figure 4

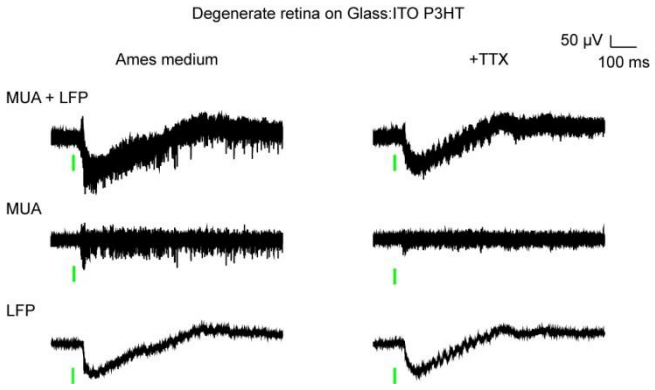

Supplementary Figure 4 | Electrophysiological activity in the RGC layer of a degenerate retina over a P3HT active layer. The top panels show the light-induced (10 ms, 4 mW/mm^2) electrophysiological activity detected in the RGC layer of a degenerate retina over a P3HT-coated Glass:ITO substrate in the absence (left) or presence (right) of TTX (1 µM). The middle and bottom panels show the MUAs and LFPs (means of 5 consecutive sweeps) extracted from the raw traces, respectively. The green bars represent the light stimulus.

Supplementary Figure 5

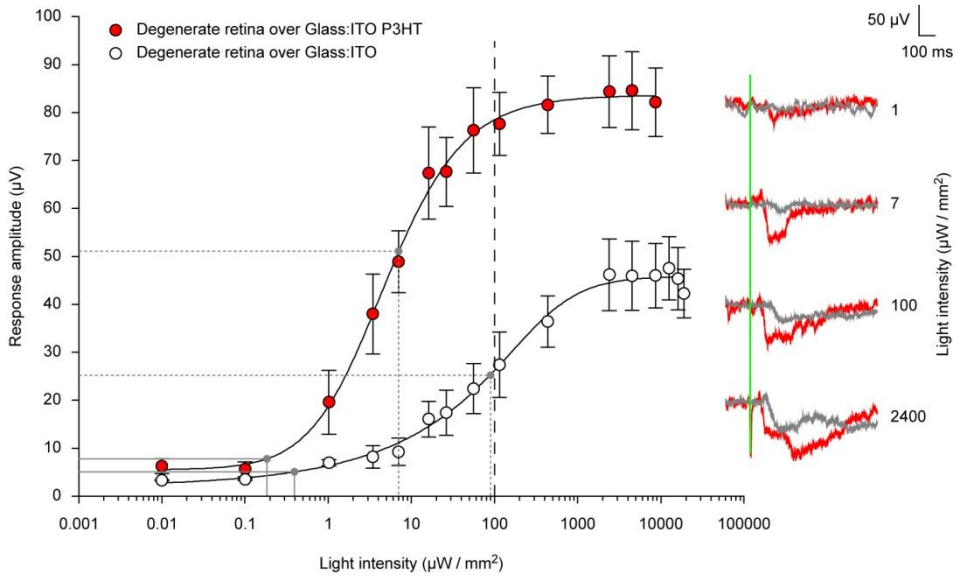

Supplementary Figure 5 | Dose-response analysis of LFP amplitudes in degenerate retinas over a P3HT active layer. Dose-response analysis of LFP amplitudes versus light intensity performed in degenerate retinas over P3HT-coated Glass:ITO (red dots, *n* = 9, means ± s.e.m.) or Glass:ITO alone (open dots, *n* = 11, means ± s.e.m.). The dashed line represents the computed maximum permissible radiant power for a chronic exposure (see Methods). Dose-response curves were fitted using a sigmoidal dose-response model. Solid grey lines represent the response threshold (10% of the maximal response), and dotted grey lines represent the average ED_{50} calculated from the fitting procedure (respectively 6.96 and 90.77 µW/mm^2). On the right, representative LFP traces obtained in the presence (red) or absence (grey) of P3HT are shown. The green bar represents the light stimulus.

Supplementary Figure 6

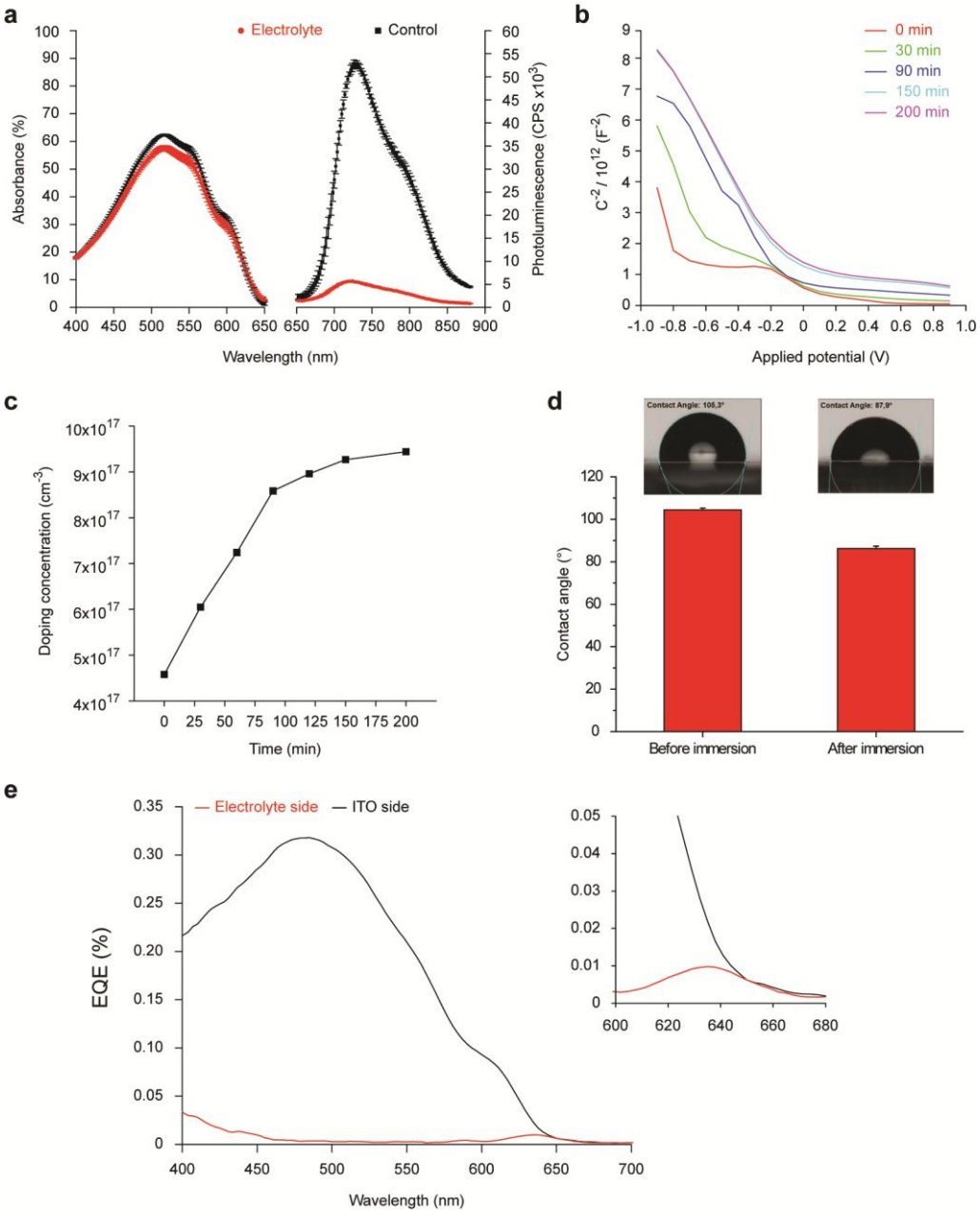

Supplementary Figure 6 | Electro-optical characterisation of a P3HT active layer in contact with the electrolyte. (**a**) Optical absorbance (left) and photoluminescence (right) spectra of P3HT films fabricated and stored under a controlled atmosphere (black, *n* = 4, means ± s.e.m.) or exposed to direct contact with electrolytic solution (NaCl, 200 mM) and continuously illuminated for 12 hr (red, *n* = 4, means ± s.e.m.). (**b**) Reverse square capacitance versus voltage measurements in the ITO/P3HT/electrolyte (NaCl, 200 mM) system. The traces are consistent with *p*-doping processes of the polymer film. The flat trace at early times shows filling of trap states at the interface. (**c**) The concentration of dopants was estimated from the slope of the linear segment. Note that the doping concentration changed over time to reach a saturation value

due to interface diffusion processes. (**d**) Mean (± s.e.m.) contact angles of distilled water drops for samples kept in an inert atmosphere (left, $n = 3$) or after immersion in electrolyte for 20 hr (right, $n = 3$). The two conditions were significantly different (Student's t-test, $P < 0.001$). The pictures on top show a characteristic drop on the polymer surface. (**e**) EQE of the system ITO/P3HT/electrolyte (NaCl, 200 mM) for light incident from the ITO side (black) or from the electrolyte side (red). The inset shows the antibatic lineshape of the photocurrent in the latter case in greater detail.